

1  
2  
3  
4  
5  
6  
7  
8  
9  
10  
11  
12  
13  
14  
15  
16  
17  
18  
19

## Standardizing thermal contrast among local climate zones at a continental scale

Xuan Chen<sup>1</sup>, Jiachuan Yang<sup>1,\*</sup>, Chao Ren<sup>2</sup>, Sujong Jeong<sup>3</sup>, Yuan Shi<sup>4</sup>

<sup>1</sup>Department of Civil and Environmental Engineering, The Hong Kong University of Science and Technology, Hong Kong, China

<sup>2</sup>Faculty of Architecture, The University of Hong Kong, Hong Kong, China

<sup>3</sup>Department of Environmental Planning, Graduate School of Environmental Studies, Seoul National University, Seoul, South Korea

<sup>4</sup>Institute of Future Cities, The Chinese University of Hong Kong, Hong Kong, China

Corresponding author: Jiachuan Yang ([cejcyang@ust.hk](mailto:cejcyang@ust.hk))

### Key Points:

- Observed temperatures over different local climate zones change with geographical conditions across China
- Characteristic temperature regimes of local climate zones are consistent at the continental scale after removing the effect of geographical conditions
- Annual mean standard thermal contrast for studied local climate zones is 0.51 °C at night and 0.22 °C during daytime.

## 20 **Abstract**

21 The Local Climate Zone (LCZ) system provides a standardized framework for intra-urban heat  
22 island studies. Yet the thermal contrast of air temperatures over different LCZs has not been  
23 examined at a large scale. Using ground-based meteorological observations in 2016, here we  
24 investigated the thermal behaviors of various LCZs over China. Measured temperatures over  
25 studied LCZs are found to have strong relations with latitude, altitude, and the distance to  
26 coastline. Thermal contrasts reduce to less than 1 °C in all seasons after removing the signal of  
27 background mean temperature determined by geographical conditions. The warmth of urban  
28 LCZs is more evident at night, with an annual mean temperature difference of 0.51 °C compared  
29 to the low-plant rural LCZ. Despite the temperature variation within individual LCZs, derived  
30 standard thermal contrasts are insensitive to changes in geographical conditions. Results reveal  
31 that consistent characteristic temperature regimes of LCZs exist at the continental scale.

## 32 **Plain Language Summary**

33 The local urban landscape has essential impacts on air temperatures above it, whether such  
34 impacts are consistent in different cities remains unclear in the literature. We used temperature  
35 data from meteorological stations to investigate the thermal behaviors of urban neighborhoods  
36 with distinct landscape properties over China. At the continental scale, air temperatures correlate  
37 strongly with geographical conditions including latitude, altitude and the distance to coastline.  
38 After removing the effect of geographical conditions, the impact of local urban landscape on air  
39 temperature is found to be consistent though with considerable variations. The warmth of urban  
40 neighborhood is more evident at night compared to during daytime. Estimated temperature  
41 differences among different urban neighborhoods and a reference rural area are generalizable for  
42 other cities in China. This study demonstrates the relation between local landscape and urban  
43 microclimate, and can provide guidance for urban planning with regards to the outdoor thermal  
44 environment.

## 45 **1 Introduction**

46 Land use/land cover conditions have significant impacts on local and regional  
47 meteorological variables. One of the most evident examples is the Urban Heat Island (UHI)  
48 effect, where urbanization leads to higher temperatures in cities compared to their surrounding  
49 countryside (Oke, 1982). Elevated temperatures in cities have adverse impacts on building  
50 energy consumption and public health during hot periods (Santamouris et al., 2015; Tomlinson et  
51 al., 2011), and past decades have seen increasing UHI studies around the world (Barreca et al.,  
52 2016; Chen & Jeong, 2018; Levermore et al., 2018; Zhou et al., 2017). The widely-used UHI  
53 intensity, defined as the urban-rural temperature difference, is nevertheless sensitive to the  
54 selection of ‘urban’ and ‘rural’ sites (Martilli et al., 2020). With dense meteorological networks  
55 deployed in recent years, high-resolution observations reveal that the intra-urban climate  
56 variability between neighborhoods can be as large as the urban-rural difference (Ramamurthy et  
57 al., 2017; Yang & Bou-Zeid, 2019). To better link local climate with landscape properties,  
58 Stewart and Oke (2012) developed the Local Climate Zone (LCZ) system that included ten built  
59 types and seven land cover types. Each LCZ type has distinguished features of surface cover,  
60 structure, material, and human activities, and has a unique characteristic air temperature regime  
61 that is most pronounced on dry, calm and clear nights (Stewart & Oke, 2012).

62 The LCZ system provides an objective framework for local-scale temperature studies in  
63 different cities. Studies have adopted the LCZ scheme with in-situ measurements to assess the  
64 intra-urban temperature variability in major metropolitan areas, including Hong Kong,  
65 Vancouver, Nagona, Uppsala, Berlin and Phoenix (Fenner et al., 2017; Stewart et al., 2014;  
66 Wang et al., 2018; Zheng et al., 2018). Reported thermal contrasts among various LCZs in  
67 studied cities evaluated the validity of the LCZ classification system, yet the analysis of air  
68 temperature was mostly conducted at the city scale and for a short study period. For example,  
69 Alexander and Mills (2014) studied the relationship between air temperature and LCZ in Dublin  
70 for one week. It is worth mentioning that surface temperature differences among LCZs have  
71 been investigated for 50 cities using satellite data (Bechtel et al., 2019). However, air  
72 temperature is of paramount interest for urban climate studies given its implications for outdoor  
73 thermal comfort and building energy consumption. Though one primary aim of the LCZ system  
74 is to standardize cross-city comparisons, air temperature contrasts among different LCZs have  
75 not been studied at a large scale.

76 Over a large spatial extent, geographical condition and atmospheric forcing vary  
77 significantly and play important roles in regulating meteorological variables. Wienert and Kuttler  
78 (2005) found the dependence of urban-rural temperature difference on latitude and suggested a  
79 larger maximum UHI intensity in high-latitude regions. Thermal contrasts among different LCZs  
80 can therefore change from city to city as local landscape only contributes partially to determining  
81 the air temperature. For example, annual mean nocturnal air temperature of LCZ 5 is about 4.4  
82 °C higher than that of LCZ D for ideal days in Szeged, Hungary (Skarbit et al., 2017), but the  
83 difference is less than 1 °C in Nanjing, China (Yang et al., 2018). The question then becomes  
84 whether the inconsistent thermal contrast between these two LCZs is caused by the difference in  
85 geographical and climatic conditions. Following the concept of the LCZ scheme, the impact of  
86 local landscape on air temperature needs to be distinguished from those of background climate  
87 and environment. This can only be achieved through large-scale analysis because geographical  
88 and climatic conditions are nearly identical at the city scale.

89 How does the characteristic temperature regime of LCZs change with geographical and  
90 climatic conditions? Is there a consistent thermal contrast among different LCZs at a large scale?  
91 How large is the temperature variability of individual LCZs compared to their thermal contrast?  
92 Answers to these questions can advance our understanding of the relation between local  
93 landscape and air temperature. To that end, we combine ground-based meteorological  
94 measurements and LCZ map to conduct a continental-scale comparative analysis over China.

## 95 **2 Materials and Methods**

### 96 **2.1 Air temperature measurement**

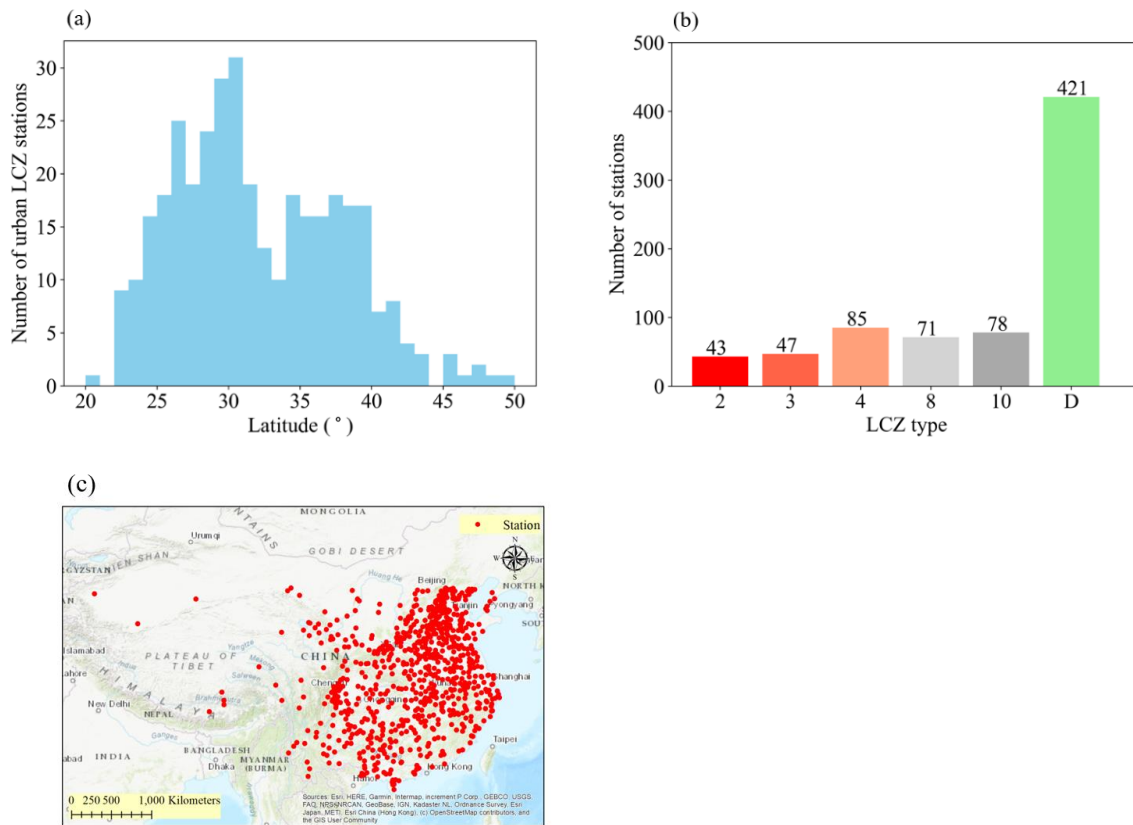
97 Hourly air temperature data measured at 2 m height above the ground level from 2131  
98 meteorological stations was collected from the National Meteorological Information Center of  
99 the China Meteorological Administration. For consistency with the LCZ map, the study period is  
100 one full year of 2016. We defined seasons as follows, spring: March - May, summer: June -  
101 August, fall: September - November, and winter: December - February. To look into thermal  
102 contrasts during the diurnal cycle, we defined daytime as 0900 - 1500 local time and nighttime as  
103 2100 - 0300 local time.

104

105 2.2 Classification of meteorological stations

106 In this study, we utilized the 2016 LCZ map of China developed using an improved  
 107 method of the World Urban Database and Portal Tool (WUDAPT). Accuracy of the LCZ  
 108 classification method has been extensively evaluated for various Chinese cities (Cai et al., 2018;  
 109 Shi et al., 2018). The LCZ map has a spatial resolution of 100 m × 100 m and includes 10 built  
 110 types (urban LCZs) and 7 land cover types. Locations of meteorological stations were overlaid  
 111 with the LCZ map to classify the air temperature measurements into different LCZ types.  
 112 Landscape homogeneity was checked to ensure measured data can represent characteristic  
 113 temperature regimes of different LCZ types. As the minimum radius to define LCZs is 200 -  
 114 500 m (Stewart & Oke, 2012), we estimated the dominant LCZ types within 3 × 3 grids and 5 ×  
 115 5 grids around each station. Only stations with matched dominant LCZ types were considered in  
 116 this study. For comparing temperature characteristics of LCZs at the continental scale, we  
 117 excluded the LCZ types with insufficient number of stations (< 40) or spatial span over China.  
 118 As a result, five urban LCZs (2: Compact mid-rise; 3: Compact low-rise; 4: Open high-rise; 8:  
 119 Large low-rise; 10: Heavy industry) and one rural LCZ (D: Low plants) were selected. To avoid  
 120 bias introduced by a small number of stations with distinct geographical conditions, we focused  
 121 on the area between 22° N – 40° N where the majority of urban LCZ stations fall (Fig. 1a). In the  
 122 end, a total of 745 stations were retained for analyses. The number of stations for each LCZ type  
 123 is shown in Fig. 1b, and the spatial distribution of studied stations is shown in Fig. 1c.

124



125

126 **Figure 1.** Distribution of meteorological stations over China. (a) Latitude distribution of urban  
 127 LCZ stations; (b) The number of stations in analyzed LCZ types; (c) Spatial

128 distribution of studied stations over China. Land use types of LCZs: 2-Compact mid-rise, 3-  
 129 Compact low-rise, 4-Open high-rise, 8-Large low-rise, 10-Heavy industry, D-Low plants.

130

131 **2.3 Multiple linear regression**

132 To estimate thermal contrasts among different LCZs at the continental scale, the  
 133 dependence of air temperature on geographical conditions must be removed. Latitude (LAT),  
 134 altitude (ALT) and the distance to coastline (DCL) are three critical parameters affecting the  
 135 background mean temperature (Linacre & Geerts, 1997). An ordinary least squares regression  
 136 analysis is then performed using these three parameters as independent variables and air  
 137 temperature as the dependent variable to establish a multiple regression model of the best fit. The  
 138 model is formulated as:

139 
$$T_{pre} = \alpha_1 LAT + \alpha_2 ALT + \alpha_3 DCL + \beta + \varepsilon, \quad (1)$$

140 where  $T_{pre}$  is the predicted background mean temperature;  $\alpha_1$ ,  $\alpha_2$ , and  $\alpha_3$  are the coefficients for  
 141 LAT, ALT, and DCL respectively;  $\beta$  is the intercept; and  $\varepsilon$  is the residual

142 **2.4 Raw and standard thermal contrast**

143 To highlight the thermal contrast among various urban neighborhoods and the rural area,  
 144 we set the rural LCZ (type D) as the reference and compute the air temperature difference  
 145 between urban LCZs ( $T_{ULCZ}$ ) and it:

146 
$$\Delta T_r = \sum(T_{ULCZ} - T_D), \quad (2)$$

147 where  $T_{ULCZ}$  and  $T_D$  are the measured temperature at individual stations belong to urban LCZs  
 148 and LCZ D. We define  $\Delta T_r$  as the raw thermal contrast, which has been employed in previous  
 149 LCZ studies (Kotharkar & Bagade, 2018; Shi et al., 2018; Verdonck et al., 2018). Note that  $\Delta T_r$   
 150 does not reveal the ‘true’ thermal contrast among different LCZs, as observed temperatures  
 151 contain the signal of background mean temperature, which is determined by geographical  
 152 conditions of stations.

153 Using the regression model detailed in section 2.3, we can remove the effect of  
 154 geographical conditions on raw thermal contrast. The impact of local landscapes can be  
 155 estimated as the deviation of measured temperature from the predicted background mean  
 156 temperature. The deviation  $\Delta T$  for each station is given by:

157 
$$\Delta T = T_{obs} - T_{pre}(LAT, ALT, DCL), \quad (3)$$

158 where  $T_{obs}$  is the observed temperature, and  $T_{pre}$  is the predicted background mean temperature  
 159 from regression models that corresponds to the geographical condition of each station.

160 Averaging  $\Delta T$  for all stations of one LCZ class yields the characteristic temperature  
 161 regime of the LCZ with respect to the background temperature. The standard thermal contrast  
 162 ( $\Delta T_s$ ) independent of geographical conditions can be computed using LCZ D as the reference  
 163 type:

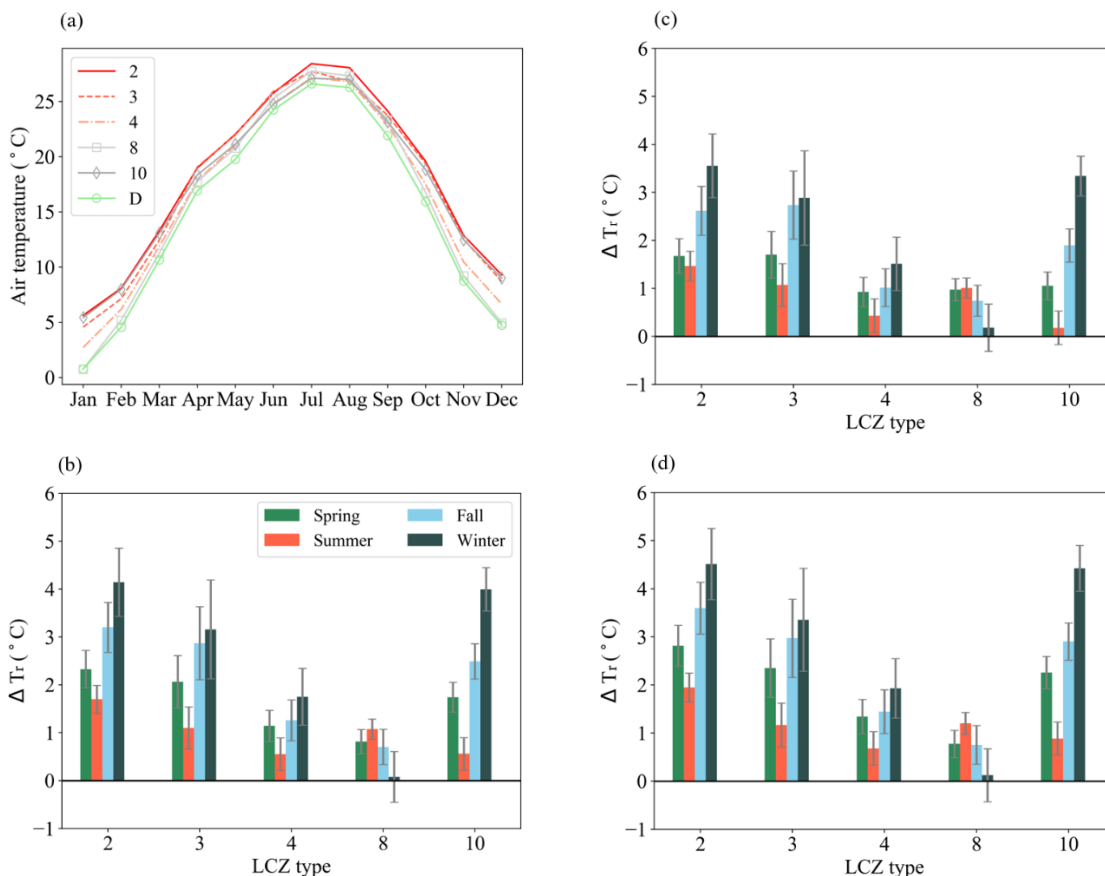
164 
$$\Delta T_s = \sum_{nULCZ}(T_{ULCZ} - T_{pre}) - \sum_{nD}(T_D - T_{pre}), \quad (4)$$

165 where nULCZ and nD denote the number of stations for each urban LCZ type and LCZ D,  
 166 respectively. Note that two  $T_{pre}$  terms on the right-hand-side of Eq. (3) will not cancel out as the  
 167 geographical condition of stations varies with LCZ types.

168 **3 Results and Discussion**

169 **3.1 Raw thermal contrast among LCZs**

170 The monthly variation of daily mean temperature for studied LCZ types is shown in Fig.  
 171 2a. Mean temperature of all LCZs is about 26.56 °C in summer and 5.59 °C in winter. The  
 172 temperature variability among studied LCZs is the smallest in summer and the largest during  
 173 winter. LCZ 2 has the highest temperature throughout the year while LCZ D has the lowest  
 174 temperature. At the annual scale, the daily mean raw thermal contrast ( $\Delta T_r$ ) is  $1.84 \pm 0.46$  °C  
 175 (mean  $\pm$  standard deviation among studied urban LCZs). Seasonal mean  $\Delta T_r$  are shown in Fig. 2.  
 176 Nighttime thermal contrasts (Fig. 2d) are found to be larger than daytime contrasts (Fig. 2c).  
 177 Summertime daily mean  $\Delta T_r$  are lower than 2 °C over all LCZs, while wintertime daily mean  
 178  $\Delta T_r$  can reach up to 4 °C over LCZs 2 and 10 (Fig. 2b). Among the studied LCZs, compact mid-  
 179 rise (LCZ 2) and heavy industry (LCZ 10) zones have the largest  $\Delta T_r$  and large low-rise  
 180 landscape (LCZ 8) has the smallest  $\Delta T_r$ . The diurnal and seasonal variations of thermal contrasts  
 181 here are consistent with previous studies, where urban-rural temperature differences found to be  
 182 more evident in winter and during nighttime (Skarbit et al., 2017; Zhou et al., 2014).  
 183 Nevertheless, results in Fig. 2 are biased by the unequal geographical conditions of stations in  
 184 different LCZs.



185

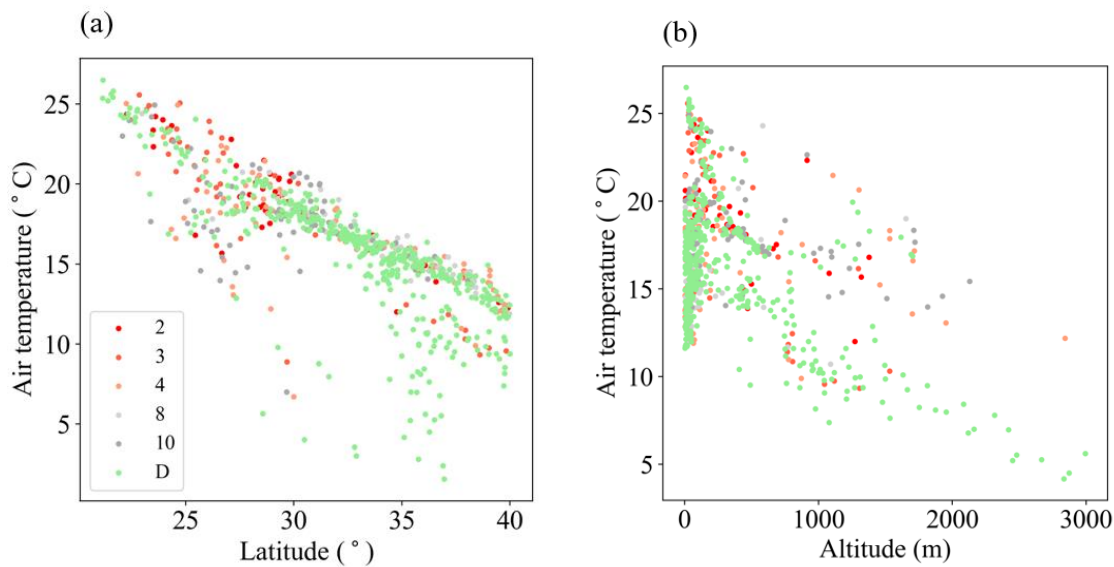
186

187 **Figure 2.** (a) Monthly variation of daily mean temperature over studied LCZ types; Raw (b)  
 188 daily mean, (c) daytime mean, (d) nighttime mean thermal contrasts ( $\Delta T_r$ ) in four seasons over  
 189 China. The error bar stands for one standard deviation from the mean of the raw thermal contrast.

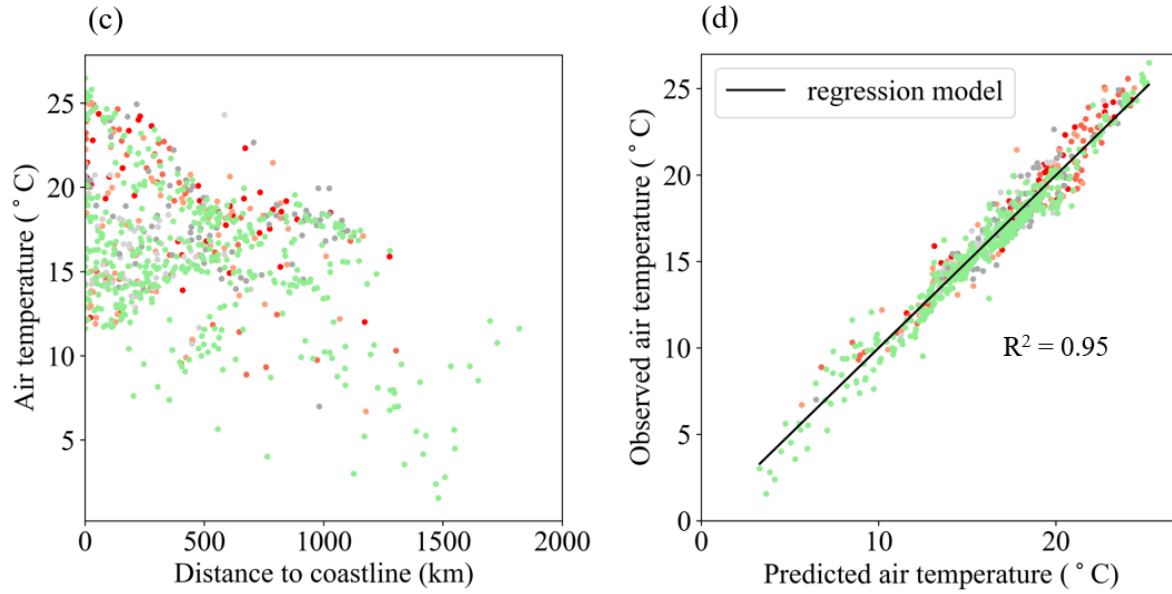
190

191 3.2 Relation between air temperature and geographical conditions

192 For each season, one multiple linear regression model is built for daily mean, daytime  
 193 mean and nighttime mean temperatures, respectively. Figure 3 shows the relations between  
 194 geographical conditions and average daily mean temperature in fall over studied stations. Air  
 195 temperatures are found to be negatively correlated with latitude, altitude, and the distance to  
 196 coastline. Predicted daily mean temperatures are compared against observations in Fig. 3d. It is  
 197 clear that the linear regression model captures the observed air temperatures in fall reasonably  
 198 well with a  $R^2$  value of 0.95. Information of the regression models for all seasons is summarized  
 199 in Table 1. In summer, fall, and winter,  $R^2$  values are greater than 0.9 for all temperatures with  
 200 RMSEs less than 1.5 °C, indicating the capacity of built regression models in reproducing the  
 201 relations between background mean temperature and geographical conditions. Note that the  
 202 regression coefficients for latitude, altitude and the distance to coastline have considerable  
 203 seasonal variations. Daily mean temperature reduces about 1 °C per degree latitude in winter, but  
 204 reduces only about 0.1 °C per degree latitude in summer. Daytime mean air temperature tends to  
 205 decrease with the distance to coastline in fall but will increase with the distance in other seasons.  
 206 Though we did not explicitly include meteorological variables in the regression analysis, the  
 207 seasonal variation of regression models implicitly contained the impact of inter-season change in  
 208 meteorological conditions on background mean temperature.



209



210

211 **Figure 3.** Relationship between (a) latitude, (b) altitude, (c) distance to the coastline and daily  
 212 mean temperature in fall; (d) comparison of predicted daily mean temperature against  
 213 observations in fall.

214

215

216 **Table 1.** Summary of regression models for daily mean, daytime (0900 – 1500 local time) mean,  
 217 and nighttime (2100 – 0300 local time) mean temperatures in four seasons.

Daily mean temperature					
	LAT coefficient (°C/degree)	ALT coefficient (°C/km)	DCL coefficient (°C/km)	$R^2$	Root mean square error (°C)
Spring	-0.45	-3.30	$1.27 \times 10^{-3}$	0.81	1.35
Summer	-0.19	-4.44	$1.59 \times 10^{-3}$	0.93	0.73
Fall	-0.68	-3.42	$-0.07 \times 10^{-3}$	0.95	0.89
Winter	-1.02	-3.05	$1.26 \times 10^{-3}$	0.95	1.20
Daytime mean temperature					
	LAT coefficient (°C/degree)	ALT coefficient (°C/km)	DCL coefficient (°C/km)	$R^2$	Root mean square error (°C)
Spring	-0.32	-3.08	$0.37 \times 10^{-3}$	0.73	1.47
Summer	-0.15	-4.39	$1.24 \times 10^{-3}$	0.92	0.78
Fall	-0.59	-3.13	$-0.90 \times 10^{-3}$	0.94	0.92
Winter	-0.92	-2.94	$0.39 \times 10^{-3}$	0.94	1.18

Nighttime mean temperature					
	LAT coefficient (°C/degree)	ALT coefficient (°C/km)	DCL coefficient (°C/km)	R <sup>2</sup>	Root mean square error (°C)
Spring	-0.54	-3.46	$1.73 \times 10^{-3}$	0.84	1.36
Summer	-0.23	-4.49	$1.67 \times 10^{-3}$	0.93	0.84
Fall	-0.74	-3.70	$0.28 \times 10^{-3}$	0.95	0.99
Winter	-1.08	-3.24	$1.58 \times 10^{-3}$	0.94	1.31

218

219

### 3.3 Standard thermal contrast among LCZs

220

221

222

223

224

225

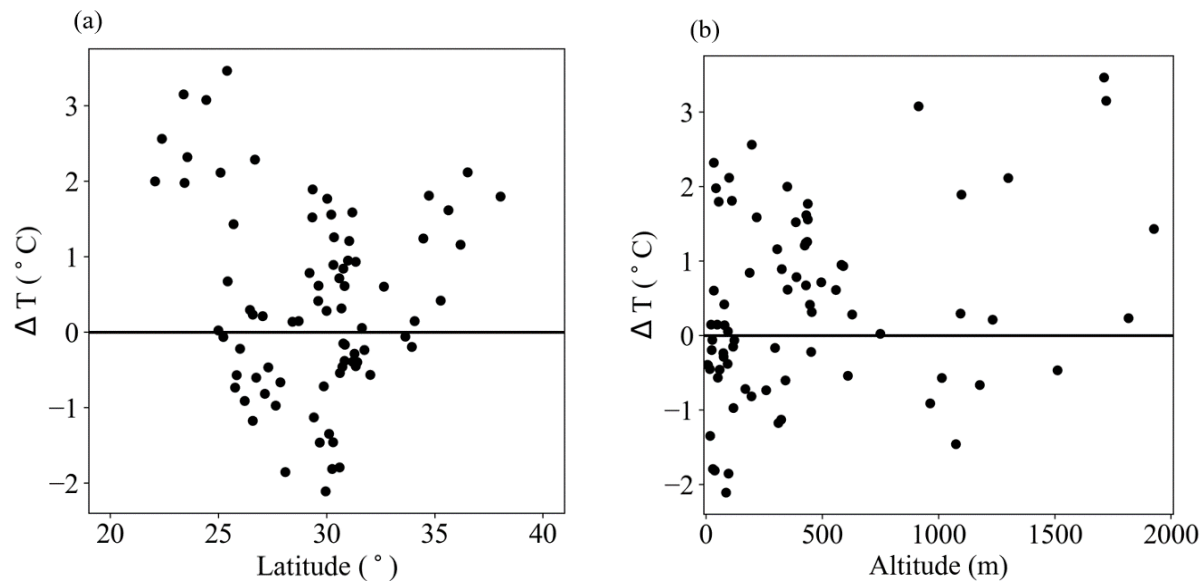
226

227

228

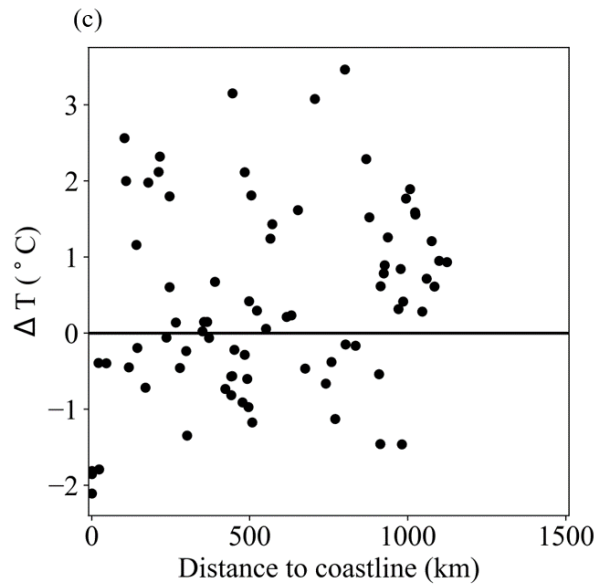
229

As  $\Delta T$  denotes only the impact of local landscape, it can be used to examine whether characteristic temperature regimes of LCZs vary with geographical conditions. Results for nighttime temperature in spring over LCZ 10 (heavy industry) is shown as an illustrative example in Fig. 4. Stations in the heavy industry LCZ can have temperature differences in the range of -2 to 3°C relative to the background temperature. Despite the large variation,  $\Delta T$  does not correlate with changes in latitude, altitude and the distance to coastline. Note that the large variation here is consistent with values reported in previous studies at the city scale (Geletič et al., 2016; Skarbit et al., 2017; Yang et al., 2018). Take the study in Nanjing, China as an example, nighttime  $\Delta T$  were found to vary between 1 - 5 °C for LCZ 2 and between -1 - 3 °C for LCZ 8.



230

231



232

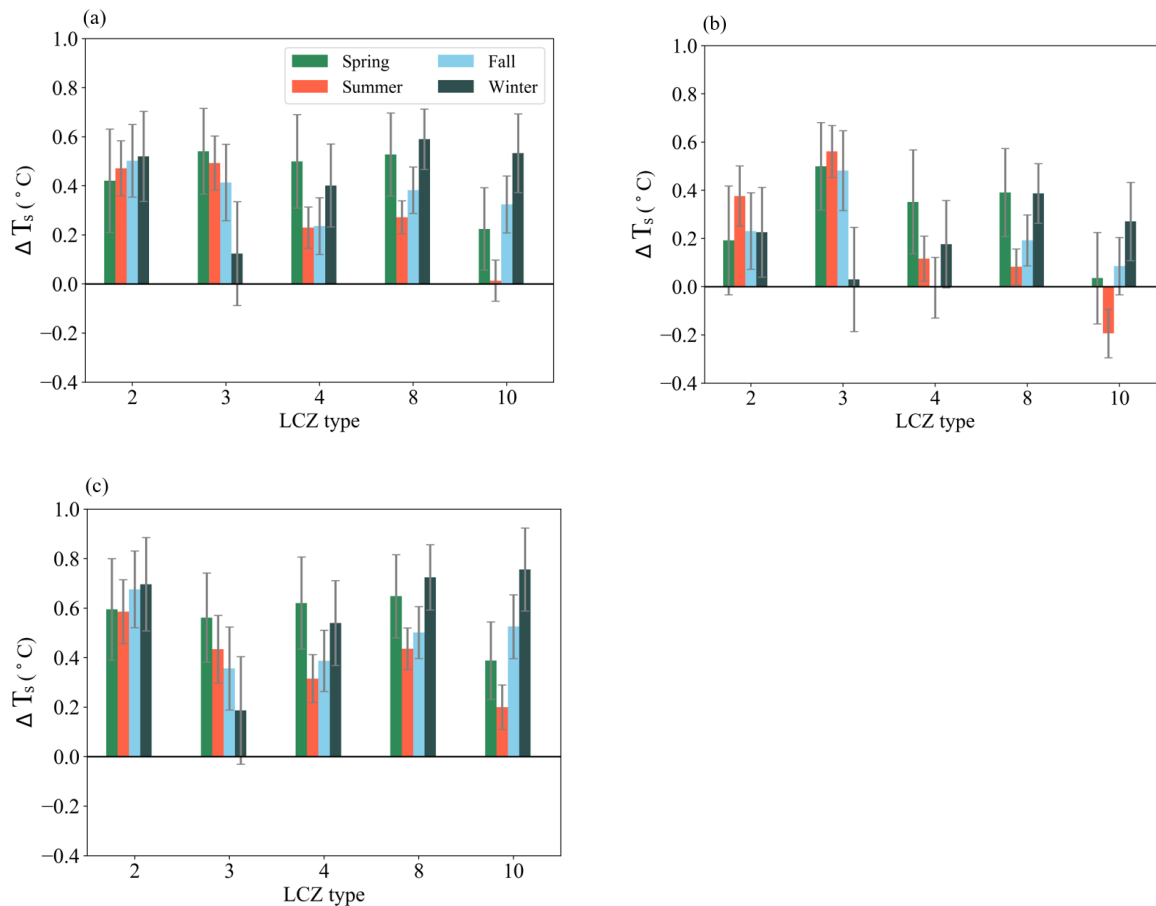
233 **Figure 4.** Distribution of the deviation of measured nighttime temperatures from the predicted  
 234 background temperature ( $\Delta T$ ) over (a) latitude, (b) altitude and (c) distance to coastline over  
 235 LCZ 10 in spring.

236

237 Figure 5 shows the average daily, daytime and nighttime mean  $\Delta T_s$  in four seasons over  
 238 China. Compared to Fig. 2, it is clear that standard thermal contrasts are smaller than raw  
 239 thermal contrasts, with all values below 1 °C. Annual mean  $\Delta T_s$  is found to be larger at night  
 240 ( $0.51 \pm 0.15$  °C, mean  $\pm$  standard deviation among studied urban LCZs, Fig. 5c) than during  
 241 daytime ( $0.22 \pm 0.15$  °C, Fig. 5b). For nighttime temperature in winter, the maximum  $\Delta T_s$  of  
 242 about 0.8 °C is found over LCZ 10 (heavy industry) and the minimum  $\Delta T_s$  is found over LCZ 3  
 243 (compact low-rise). Contrarily, large daytime thermal contrasts are observed over LCZ 3 in  
 244 summer, while a small negative value occurs over LCZ 10. Daily mean  $\Delta T_s$  remain relatively  
 245 constant across four seasons over LCZ 2 (compact mid-rise). Results here clearly demonstrates  
 246 the different behaviors of characteristic temperature regimes over studied LCZ types in response  
 247 to seasonal and diurnal variations of meteorological conditions.

248 We would like to point out that mean variation of  $\Delta T_s$  within individual LCZs is 0.15 °C  
 249 (error bars in Fig. 5) is as large as the standard deviation of  $\Delta T_s$  among studied 5 LCZ types.  
 250 This indicates that when one LCZ has higher mean temperatures than others, some stations  
 251 belong to that LCZ could have lower temperatures. Such variation is partly due to the structure  
 252 of the LCZ system, where the ranges of landscape properties used for classifying different LCZs  
 253 overlap. For example, LCZ 2 and LCZ 3 have the same building surface fraction threshold (40%  
 254 - 60%) and similar aspect ratio ranges (0.75-2 for LCZ 2 and 0.75-1.5 for LCZ 3). Though many  
 255 other parameters are involved in the LCZ classification scheme, overlapped ranges inevitably  
 256 result in large variability in the characteristic temperature regime of LCZs and consequently their  
 257 thermal contrast.

258 In spite of the considerable variation, standard thermal contrasts among different LCZs  
 259 estimated in this study support the validity of the LCZ scheme at the continental scale. Though  
 260 the magnitudes of standard thermal contrasts are not large, we would like to emphasize that  
 261 estimated  $\Delta T_s$  represent the influence on air temperature solely by local urban landscape and do  
 262 not vary with geographical conditions. Wang et al. (1990) removed the bias related to  
 263 geographical conditions and reported a mean UHI intensity of 0.23 °C during 1954 – 1983 over  
 264 entire China. Using observed temperature data in 2016, we find the annual mean air temperature  
 265 over studied urban LCZs is 0.39 °C higher than that over rural areas with low plants. The result  
 266 indicates that continuous urbanization between 1983 and 2016 has further increased urban-rural  
 267 temperature difference over China.



268

269

270 **Figure 5.** Standard (a) daily mean, (b) daytime mean, (c) nighttime mean thermal contrast ( $\Delta T_s$ )  
 271 in four seasons over China. The error bar stands for one standard deviation from the mean of the  
 272 standard thermal contrast.

273

#### 274 4 Conclusions

275 In this study, we make the first attempt to examine the characteristic temperature regimes  
 276 of different LCZs across China. Using low plants as the reference LCZ type, raw thermal  
 277 contrasts directly from station measurements are found to be up to 4 °C in winter. After  
 278 removing the signal of background mean temperature, the standard thermal contrasts become

279 less than 1 °C for all seasons. Results show that the warmth of urban LCZs is more evident  
280 during nighttime, with the maximum effect observed in compact mid-rise zones. The impact of  
281 local urban landscape on air temperature over studied LCZ types are consistent at the continental  
282 scale and do not change with geographical conditions. Estimated standard thermal contrasts in  
283 this study are generalizable for microclimate in other Chinese cities. Large standard thermal  
284 contrast with low variations suggests consistently high air temperatures in compact mid-rise  
285 neighborhoods (LCZ 2) throughout the year. On the other hand, open high-rise neighborhoods  
286 (LCZ 4) have large  $\Delta T_s$  in winter and low  $\Delta T_s$  in summer, which is desirable in terms of building  
287 energy consumption and outdoor thermal comfort. The findings here thus could provide  
288 guidance for urban planning.

289 The reduction in sensor cost and the ease of data communication have allowed us to  
290 monitor the urban thermal environment at a much finer resolution. A recent study showed the  
291 critical role of intra-urban climate variability on modifying residents' health risk under extreme  
292 events (Yang et al., 2019). The LCZ system provides a good standard for classifying urban  
293 neighborhoods with heterogeneous landscape, and facilitates the design and development of  
294 urban monitoring networks. Due to data availability, our analysis only focuses on air  
295 temperature. Future studies shall investigate the characteristic regime of other variables over  
296 different LCZs, such as air humidity and wind speed. Another limitation of this study is the  
297 neglect of meteorological conditions in the estimation of standard thermal contrasts. The relation  
298 between temperature variability and meteorological conditions in different LCZs is worth further  
299 investigation.

### 300 **Acknowledgments, Samples, and Data**

301 This work was supported by the Hong Kong Research Grants Council funded project 16204220.  
302 Due to data policy in China, original hourly temperature data at 2739 stations are not available  
303 via a public repository. Anyone of interest could contact China Meteorological Administration  
304 (<http://www.cma.gov.cn/en2014/>) for detailed information of data acquisition. Seasonal daily,  
305 daytime and nighttime mean air temperature data in this study is available at: [https://doi.org/](https://doi.org/10.5281/zenodo.3940212)  
306 [10.5281/zenodo.3940212](https://doi.org/10.5281/zenodo.3940212). The study of LCZ data development was partially supported by the  
307 Vice-Chancellor's One-off Discretionary Fund of The Chinese University of Hong Kong.

### 308 **References**

- 309 Alexander, P. J., & Mills, G. (2014). Local climate classification and Dublin's urban heat island.  
310 *Atmosphere*, 5(4), 755-774. doi: 10.3390/atmos5040755
- 311 Barreca, A., Clay, K., Deschenes, O., Greenstone, M., & Shapiro, J. S. (2016). Adapting to  
312 climate change: The remarkable decline in the US temperature-mortality relationship over the  
313 twentieth century. *Journal of Political Economy*, 124(1), 105-159. doi: 10.1086/684582
- 314 Bechtel, B., Demuzere, M., Mills, G., Zhan, W., Sismanidis, P., Small, C., & Voogt, J. (2019).  
315 SUHI analysis using local climate Zones—A comparison of 50 cities. *Urban Climate*, 28,  
316 100451. doi: 10.1016/j.uclim.2019.01.005
- 317 Cai, M., Ren, C., Xu, Y., Lau, K. K., & Wang, R. (2018). Investigating the relationship between  
318 local climate zone and land surface temperature using an improved WUDAPT methodology—A

- 319 case study of Yangtze river delta, China. *Urban Climate*, 24, 485-502. doi:  
320 10.1016/j.uclim.2017.05.010
- 321 Chen, X., & Jeong, S. J. (2018). Shifting the urban heat island clock in a megacity: a case study  
322 of Hong Kong. *Environmental Research Letters*, 13(1), 014014. doi: 10.1088/1748-9326/aa95fb
- 323 Fenner, D., Meier, F., Bechtel, B., Otto, M., & Scherer, D. (2017). Intra and inter local climate  
324 zone variability of air temperature as observed by crowdsourced citizen weather stations in  
325 berlin, Germany. *Meteorologische Zeitschrift*, 26, 525-547. doi: 10.1127/metz/2017/0861
- 326 Geletič, J., Lehnert, M., & Dobrovolný, P. (2016). Land surface temperature differences within  
327 local climate zones, based on two central European cities. *Remote Sensing*, 8(10), 788. doi:  
328 10.3390/rs8100788
- 329 Kotharkar, R., & Bagade, A. (2018). Evaluating urban heat island in the critical local climate  
330 zones of an Indian city. *Landscape and Urban Planning*, 169, 92-104. doi:  
331 10.1016/j.landurbplan.2017.08.009
- 332 Levermore, G., Parkinson, J., Lee, K., Laycock, P., & Lindley, S. (2018). The increasing trend of  
333 the urban heat island intensity. *Urban Climate*, 24, 360-368. doi: 10.1016/j.uclim.2017.02.004
- 334 Geerts, B., & Linacre, E. (1997). *Climates and weather explained*. Abingdon, Routledge.
- 335 Martilli, A., Krayenhoff, E. S., & Nazarian, N. (2020). Is the urban heat island intensity relevant  
336 for heat mitigation studies? *Urban Climate*, 31, 100541. doi: 10.1016/j.uclim.2019.100541
- 337 Oke, T. R. (1982). The energetic basis of the urban heat island. *Quarterly Journal of the Royal  
338 Meteorological Society*, 108(455), 1-24. doi: 10.1002/qj.49710845502
- 339 Ramamurthy, P., González, J., Ortiz, L., Arend, M., & Moshary, F. (2017). Impact of heatwave  
340 on a megacity: an observational analysis of New York City during July 2016. *Environmental  
341 Research Letters*, 12(5), 054011. doi: 10.1088/1748-9326/aa6e59
- 342 Santamouris, M., Cartalis, C., Synnefa, A., & Kolokotsa, D. (2015). On the impact of urban heat  
343 island and global warming on the power demand and electricity consumption of buildings—A  
344 review. *Energy and Buildings*, 98, 119-124. doi: 10.1016/j.enbuild.2014.09.052
- 345 Shi, Y., Lau, K. K., Ren, C., & Ng, E. (2018). Evaluating the local climate zone classification in  
346 high-density heterogeneous urban environment using mobile measurement. *Urban Climate*, 25,  
347 167-186. doi: 10.1016/j.uclim.2018.07.001
- 348 Skarbit, N., Stewart, I. D., Unger, J., & Gál, T. (2017). Employing an urban meteorological  
349 network to monitor air temperature conditions in the 'local climate zones' of Szeged, Hungary.  
350 *International Journal of Climatology*, 37, 582-596. doi: 10.1002/joc.5023

- 351 Stewart, I. D., Oke, T. R., & Krayenhoff, E. S. (2014). Evaluation of the ‘local climate  
352 zone’ scheme using temperature observations and model simulations. *International Journal of*  
353 *Climatology*, 34(4), 1062-1080. doi: 10.1002/joc.3746
- 354 Stewart, I. D., & Oke, T. R. (2012). Local climate zones for urban temperature studies. *Bulletin*  
355 *of the American Meteorological Society*, 93(12), 1879-1900. doi: 10.1175/BAMS-D-11-00019.1
- 356 Tomlinson, C. J., Chapman, L., Thornes, J. E., & Baker, C. J. (2011). Including the urban heat  
357 island in spatial heat health risk assessment strategies: A case study for Birmingham, UK.  
358 *International Journal of Health Geographics*, 10(1), 42. doi: 10.1186/1476-072X-10-42
- 359 Verdonck, M., Demuzere, M., Hooyberghs, H., Beck, C., Cyrus, J., Schneider, A., . . . Van  
360 Coillie, F. (2018). The potential of local climate zones maps as a heat stress assessment tool,  
361 supported by simulated air temperature data. *Landscape and Urban Planning*, 178, 183-197. doi:  
362 10.1016/j.landurbplan.2018.06.004
- 363 Wang, C., Middel, A., Myint, S. W., Kaplan, S., Brazel, A. J., & Lukasczyk, J. (2018). Assessing  
364 local climate zones in arid cities: The case of Phoenix, Arizona and Las Vegas, Nevada. *ISPRS*  
365 *Journal of Photogrammetry and Remote Sensing*, 141, 59-71. doi:  
366 10.1016/j.isprsjprs.2018.04.009
- 367 Wang, W., Zeng, Z., & Karl, T. R. (1990). Urban heat islands in China. *Geophysical Research*  
368 *Letters*, 17(13), 2377-2380 doi: 10.1029/GL017i013p02377
- 369 Wienert, U., & Kuttler, W. (2005). The dependence of the urban heat island intensity on  
370 latitude—a statistical approach. *Meteorologische Zeitschrift*, 14(5), 677-686. doi: 10.1127/0941-  
371 2948/2005/0069
- 372 Yang, J., & Bou-Zeid, E. (2019). Designing sensor networks to resolve spatio-temporal urban  
373 temperature variations: fixed, mobile or hybrid?. *Environmental Research Letters*, 14(7),  
374 074022. doi: 10.1088/1748-9326/ab25f8
- 375 Yang, J., Hu, L., & Wang, C. (2019). Population dynamics modify urban residents’ exposure to  
376 extreme temperatures across the United States. *Science advances*, 5(12), eaay3452. doi:  
377 10.1126/sciadv.aay3452
- 378 Yang, X., Yao, L., Jin, T., Peng, L. L., Jiang, Z., Hu, Z., & Ye, Y. (2018). Assessing the thermal  
379 behavior of different local climate zones in the Nanjing metropolis, China. *Building and*  
380 *Environment*, 137, 171-184. doi: 10.1016/j.buildenv.2018.04.009
- 381 Zheng, Y., Ren, C., Xu, Y., Wang, R., Ho, J., Lau, K., & Ng, E. (2018). GIS-based mapping of  
382 local climate zone in the high-density city of Hong Kong. *Urban Climate*, 24, 419-448. doi:  
383 10.1016/j.uclim.2017.05.008
- 384 Zhou, B., Rybski, D., & Kropp, J. P. (2017). The role of city size and urban form in the surface  
385 urban heat island. *Scientific reports*, 7(1), 1-9. doi: 10.1038/s41598-017-04242-2

386 Zhou, D., Zhao, S., Liu, S., Zhang, L., & Zhu, C. (2014). Surface urban heat island in China's 32  
387 major cities: Spatial patterns and drivers. *Remote Sensing of Environment*, 152, 51-61. doi:  
388 10.1016/j.rse.2014.05.017

389

390